EPHA2-dependent Ephrin-B1 signaling supports self-renewal ability and recurrence of oral cancer

Reshma Raj R[1,2], Soumya Krishnan U[1], Geetha Shanmugam[1], Nandini Datta[1], Jiss Maria Louis[1], Ravichandran Damodaran Jeyaram[1], Keshava K Datta[3], Harsha Gowda[3], Meghna Sarkar[1], Madhumathy G Nair[4], Jyothy S Prabhu[4], Hafsa Shabeer[4], Balagopal P G[5, 6], Thameem A[5], Alan Jose[5], and Tessy Thomas Maliekal[1, 2]*

[1]Cancer Research, Rajiv Gandhi Centre for Biotechnology, Thiruvananthapuram, Kerala, India, 695014
[2] Regional Centre for Biotechnology, Faridabad, Haryana, India,121001

[3]Institute of Bioinformatics, Bangalore, Karnataka, India, 560066

[4]Division of Molecular Medicine, St. John's Research Institute, St John's National Academy of Health Sciences, Bangalore, India, 560034.
[5]Cochin Cancer Research Centre, Cochin, Kerala, India, 683503
[6] Surgical Oncology, Regional Cancer Centre, Thiruvananthapuram, Kerala, India, 695011.

*To whom correspondence should be addressed

Cancer Research,
Rajiv Gandhi Centre for Biotechnology
Thiruvananthapuram,
Kerala, India-695014
E-mail: tessy@rgcb.res.in
Ph: +91-471-2529510
https://orcid.org/0000-0002-7311-7950

Key words

cancer stem cells/EPHA2/Ephrin-B1/ Eph-Ephrin signaling/oral cancer/ recurrence/ self-renewal ability

ABSTRACT

As self-renewal of cancer cells is the underlying cause of recurrence and poor prognosis, understanding its molecular determinants is important. Despite the established role of Ephrin-B1 in the regulation of normal stem cells, its role in the self-renewal of cancer cells is poorly explored. Here, using proteomic approach, we report that Ephrin-B1 and its signaling is critical for the self-renewal of oral cancer cells. Further, biochemical analyses revealed that the expression of Ephrin-B1 and EPHA2, a known regulator of cancer stem cells (CSCs), are up-regulated in parallel to the enrichment of self-renewal. Unlike the normal context, as reported, this aberrant upregulation enables their *cis*-interaction, leading to the phosphorylations of EphrinB1 Y324/329 and Y317. Our *in vitro* and *in vivo* functional analyses confirmed the role of Ephrin-B1-EPHA2 signaling in enriching CSCs. Using mouse orthotopic models, we show that abrogation of the ligand, receptor or both results in better prognosis. Moreover, the results of the *in silico* and immunohistochemical analysis of oral cancer samples reinforced the critical involvement of this signaling in the recurrence of the disease.

Introduction

Eph/Ephrin signaling is a bidirectional signaling, which is mediated through membrane bound Eph receptors and Ephrin ligands. Eph receptors are tyrosine kinases, which are classified into A or B based on the similarity in the sequence. Humans have nine EphA receptors, five EphB receptors, five Ephrin-A ligands with glycosylphosphatidylinositol (GPI) linkage, and three Ephrin-B ligands with transmembrane region. Although the type-A receptors interact with type-A ligands, and B-receptors with B-ligands, cross interactions are also reported (Pasquale, 2010). When the receptor molecule of one cell interacts with the ligand molecule on the neighboring cell, a *trans* interaction occurs, which may lead to the signaling events in the receptor bearing cell (forward signaling) and the ligand bearing cell (reverse signaling). At the same time, the ligand and receptor of the same cell can also interact, i.e., *cis* interaction, the consequence of which is not well characterized (Pasquale, 2024). Eph/Ephrin signaling contributes to varied context dependent functions *via* diverse range of receptor-ligand combinations, *cis* or *trans* interactions, bidirectional or unidirectional signaling, and Ephrin-independent non-canonical signaling of Eph receptors or Eph-independent signaling of Ephrin ligands (Pasquale, 2024). Given the complexity of the system, the downstream pathway in each of these contexts are not resolved. However, the phosphorylation of some of the residues of the receptors and the ligands are reported. Yet, there is considerable lacunae in our understanding of how the phosphorylations of the receptors and ligands lead to the specific effect. With its different layers of intricacy, this signaling can tightly regulate different developmental processes as well as cancer. During development, it is known to regulate axon growth (Mann *et al*, 2004), tissue patterning (Medori *et al*, 2020), tissue boundary formation (Mellitzer *et al*, 1999), migration of stem cells (Arthur *et al*, 2009; Goichberg *et al*, 2011), and stem cell maintenance (Arthur *et al*, 2019; Batlle *et al*, 2002; Chen *et al*, 2015; Ottone

et al, 2014). Complementary to these developmental processes, several tumorigenic properties like, proliferation, apoptosis, angiogenesis, metastasis, and immune modulation are also regulated by Eph/Ephrin pathway (Pasquale, 2024). Several members of this family are shown to be involved in regulating various aspects of malignancy.

Ephrin-B1 is a ligand typically shown to bind with EphB1 or EphB2 receptor, and is well-explored in the context of stem cells. Ephrin-B1-mediated EphB signaling is shown to be important for the proliferation of dental pulp stem cells, and tissue repair (Stokowski *et al*, 2007; Zhu *et al*, 2015). Similarly, neural progenitor compartment is also regulated by this signaling (Catchpole & Henkemeyer, 2011). The role of this signaling is extensively studied in the mouse intestinal crypts, where, the reverse gradient of EphB2/B3 and Ephrin-B1 expression, and the signaling there by regulates the stem cell compartment position, proliferation and differentiation (Batlle *et al.*, 2002). In spite of its well-established role in normal stem cell regulation, its contribution in cancer stem cells (CSCs) and cancer is poorly explored. However, a correlative analysis has shown that Ephrin-B1 is a marker for aggressiveness of bladder cancer (Mencucci *et al*, 2020). Recently, we have reported that Ephrin-B1 ablation can reduce the self-renewal ability of oral cancer stem cells *in vitro*, implicating its role in oral cancer (Dharmapal *et al*, 2021). One of the Eph family members reported to regulate CSCs is EPHA2. It is shown to regulate CSCs of glioblastoma (Binda *et al*, 2012), non-small cell lung carcinoma (Song *et al*, 2014), nasopharyngeal carcinoma (Li *et al*, 2019) and oral squamous cell carcinoma (OSCC) (Bai *et al*, 2024). Even though the role of EPHA2 receptor in CSCs is well reported, ligand molecule that interacts with EPHA2 in CSCs is not identified.

The current study was initiated with the investigation of the signaling pathways, their ligands and receptors regulating self-renewal of oral cancer cells. Since our results pointed out the importance of Ephrin-B1 and the signaling mediated by this ligand, we explored the role of this signaling in regulating the self-renewal ability of oral cancer cells, which leads to recurrence and poor prognosis. Here, we present the evidence for the interaction of Ephrin-B1 with EPHA2. Further, we explored the possibility of this Ephrin-B1-EPHA2 interaction in the phosphorylation of the ligand and the receptor to mediate downstream signaling. The significance of this signaling in the regulation of oral cancer prognosis was validated using mouse models and OSCC primary samples.

Results

Eph/Ephrin signaling is regulated in parallel to the enrichment of self-renewing cancer cells in oral cancer

Since self-renewing cancer cells are the culprit of cancer properties like tumor initiation, metastasis and recurrence, we explored the pathways regulating self-renewal ability in oral cancer cells. The surface molecules, usually, the receptors and ligands of different pathways critically regulate the properties of cancer cells. Sphere culture is an established way of enriching the self-renewing population, which we confirmed with sustained sphere formation efficiency up to three passages, as well as increased soft agar colony formation, increased expression of stem cell markers like *ALDH1A1*, *BMI1, KLF4, NANOG* and *OCT4A* in sphere culture compared to monolayer cells (Fig. S1A-E). To identify the surface molecules and pathways of self-renewal in oral cancer, we performed a proteomic analysis of the surface molecules and a phosphoproteomic analysis, using sphere culture in comparison to monolayer cells after SILAC labelling (Fig. S2A-

B). We identified 148 surface molecules to be specifically enriched in sphere culture (Fig. 1A, Table S1). Up-regulation of some of the surface molecules obtained from the analysis was confirmed using western-blotting of the membrane preparation (Fig. 1B-C).

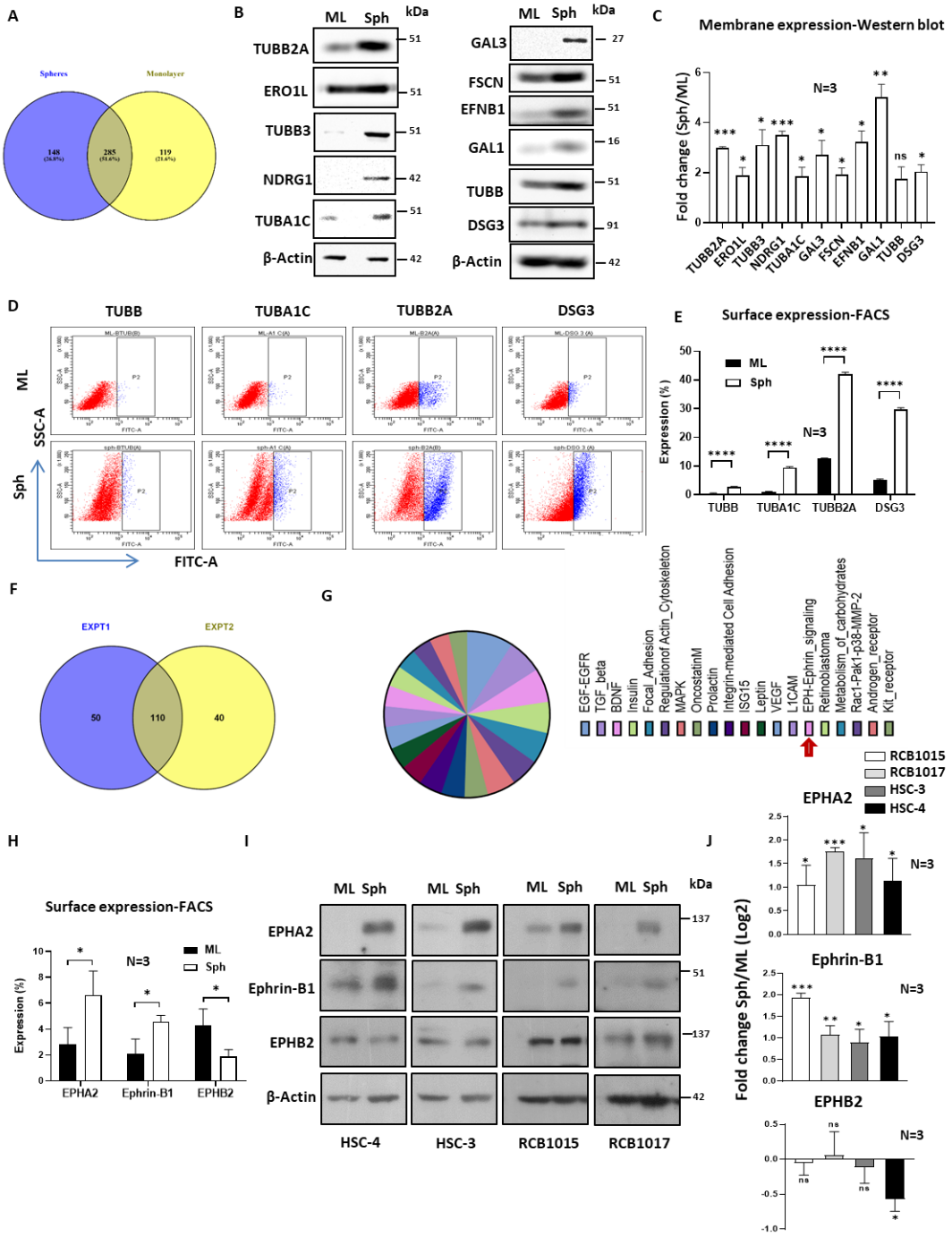

Figure 1.Eph/Ephrin signaling is regulated in parallel to the enrichment of self-renewing cancer cells in oral cancer. A, SILAC-labelled HSC-4 oral cancer cells were grown in monolayer and sphere culture for 6 days. Then we did membrane preparation followed with a SILAC based proteomic analysis using LTQ–OrbitrapVelos ETD mass spectrometer. The Venn diagram shows the number of surface molecules enriched in spheres (148), monolayer (119), and common in both (285). B, Some of the molecules obtained from proteomic analysis were confirmed in western-blotting using lysates of 6-Day spheres and monolayer of HSC-4 cells. C, data plotted with mean ± SD values from 3 independent experiments. D, E, HSC-4 Cells were grown in monolayer and sphere condition for 3 days, and were used for FACS analysis to check surface expression of some of the molecules under non-permeabilizing condition. The percentage of cells showing surface expression of the indicated molecules in monolayer and spheres were plotted as mean ± SD values from 3 replicates. F, As explained before, SILAC-labelled HSC-4 oral cancer cells were grown in monolayer and sphere culture for 6 days, and were used for phosphoproteomic analysis after enrichment of phosphopeptides using TiO_2 beads. The pathways differentially regulated in spheres in the two independent experiments were shown. We identified 110 unique pathways differentially regulated in spheres. G. Among the 110 unique pathways identified, 50 pathways were important for the regulation of self-renewal of normal stem cells or CSCs. From that 50 pathways, the top 20 pathways were selected based on the highest number of molecules detected, and were represented in the pie chart. One among them was Eph-Ephrin signaling. H. HSC-4 cells were grown in monolayer and sphere for 3 days were used for FACS analysis for surface expression of EPHA2, Ephrin-B1 and EPHB2 as described before. I, Oral cancer cells were grown in monolayer and sphere culture for 3 days. Then we did western-blotting analysis to check expression of EPHA2, Ephrin-B1 and EPHB2 in the whole cell lysate. J, Data plotted as mean ± SD values from 3 independent experiments. Statistical analysis was done by paired-two tailed students t-test. *, **, ***, **** represents $p<0.05$, $p<0.01$, $p<0.001$ and $p<0.0001$, respectively.

The surface localization of a few molecules (TUBB, TUBA1C, TUBB2A, DSG3, TUBB4B, EFNB1) were confirmed using immunofluorescence and FACS analysis (Fig. S3A, Fig. 1D-E). One of the molecules found to be enriched in spheres was Ephrin-B1, which is a membrane bound ligand involved in Eph/Ephrin signaling. Further, to identify critical pathways, we did two independent phosphoproteomic analyses using oral cancer cells, HSC-4. The peptides and proteins identified in replicate 1 and 2 are given in Tables S2-4. Our duplicate analysis identified 110 unique pathways differentially regulated in spheres compared to monolayer (Fig. 1F, Table S5). From the 110 pathways, we selected 50 pathways that are shown to be linked to self-renewal either in normal

or cancer contexts are given in Table S6 and Fig 1G. Phosphorylation of some of the molecules were confirmed using western-blotting (Fig. S3B).

Supporting the observation of surface enrichment of Ephrin-B1 in our surface proteomic analysis, we observed that Eph/Ephrin signaling is one of the signaling pathways differentially regulated in sphere condition. Out of the 17 molecules involved in this pathway that were differentially phosphorylated upon sphere condition, the ligands and receptors involved were EPHA2, EPHB2 and Ephrin-B1 (Table S7). While the ligand Ephrin-B1 and receptor EPHA2 showed hyperphosphorylation, EPHB2 exhibited hypophosphorylation upon sphere formation (Table S7, Fig. S3C). The results suggested that self-renewal enrichment is positively correlated to Ephrin-B1 and EPHA2 whereas it showed a negative correlation with EPHB2. To confirm the surface expression of the receptors and ligands, which will lead to a signaling, we did a FACS analysis. In accordance with the phosphorylations observed, the surface expression of Ephrin-B1 and EPHA2 increased with a concomitant decrease in EPHB2 surface expression in the sphere condition (Fig. 1H, Fig. S3D). To explore the significance of this observation in more oral cancer cells, we took 4 oral cancer cell lines to analyze the differential expression in spheres and monolayer cells. EPHA2 receptor and Ephrin-B1 ligand exhibited enrichment in spheres across all the cell lines while EPHB2 receptor showed no significant change in the total expression except in HSC-4 cells, where it showed a significant reduction (Fig. 1I-J). Taken together, our results show that there is an increased surface expression of the ligand Ephrin-B1 and the receptor EPHA2, upon the induction of self-renewal in oral cancer cells. Thus the chance of interaction of EphrinB1 to EPHA2 is more in spheres compared to monolayer.

Ephrin-B1 engages with EPHA2, and leads to differential phosphorylation in the self-renewal enriched sphere condition

As our results indicated that in sphere condition, Ephrin-B1 might interact with EPHA2, we performed co-immunoprecipitation (Co-IP) experiment to check whether the ligand binds to EPHA2 or EPHB2. As expected from the surface expression pattern, the level of Ephrin-B1 and its interaction with EPHA2 was more in spheres compared to monolayer cells (Fig. 2A). At the same time, Ephrin-B1 did not interact with EPHB2 in sphere or monolayer (Fig. 2A). Then, the interaction of Ephrin-B1 ligand with EPHA2 receptor was validated using reverse Co-IP (Fig. 2B).

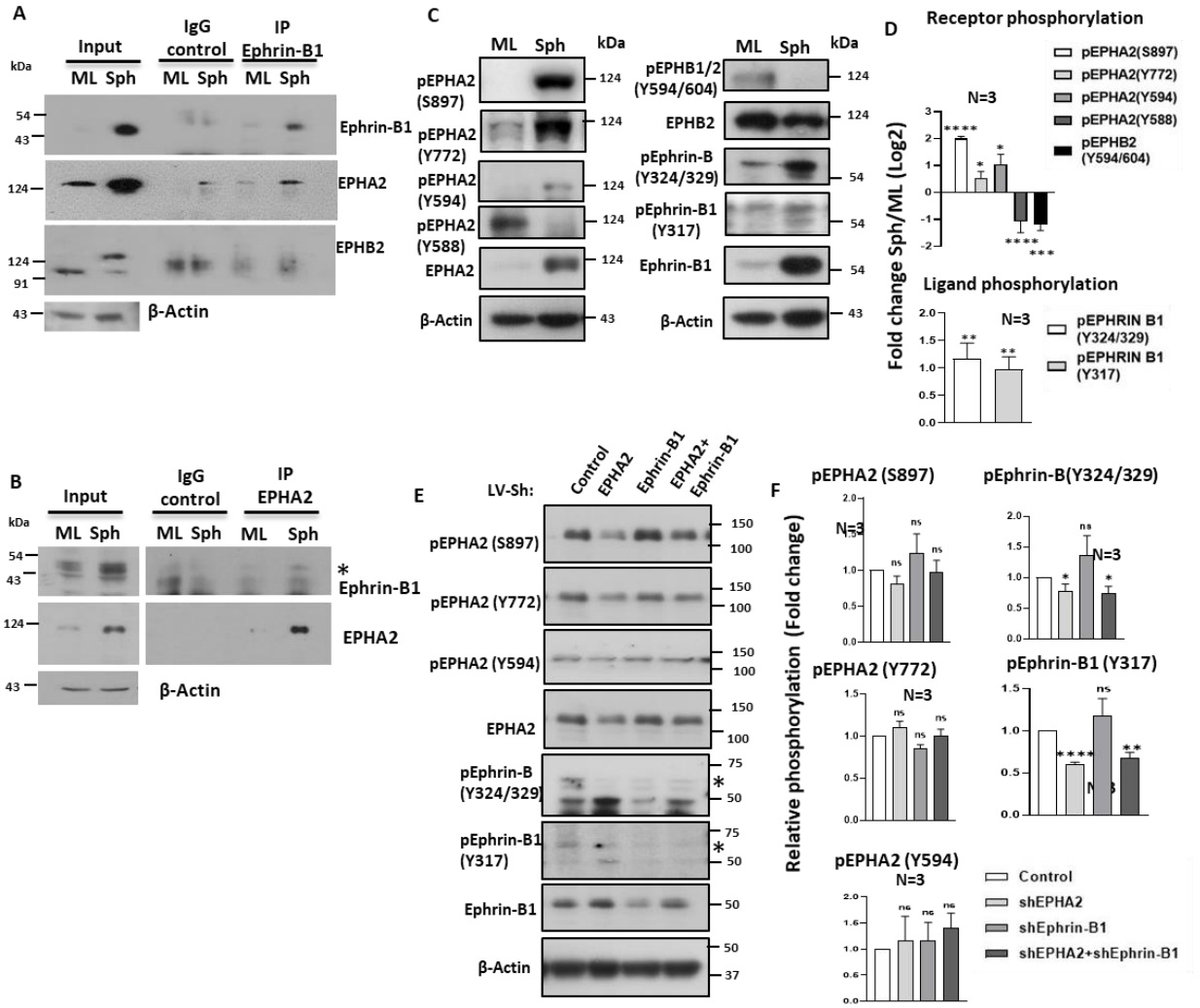

Figure 2 Ephrin-B1 engages with EPHA2, and leads to differential phosphorylation in the self-renewal enriched sphere condition. HSC-4 cells were grown as monolayer or spheres, and were used for all the experiments. A, Co-IP of mouse Ephrin-B1 (3µg) along with mouse IgG as a control and 7% input. The eluate was probed for the indicated molecules. B, Reverse Co-IP experiment was performed with Rabbit EPHA2 (3µg) antibody, Rabbit IgG and 7% input. C, western-blotting in the whole cell lysate to check phosphorylation of indicated molecules, and its quantification. D, phosphorylation was calculated after normalizing with β-Actin. Then the fold change in spheres compared to monolayer is plotted as mean ± SD values from 3 independent experiments. E, Western-blotting in the whole cell lysate of 3D-spheres to check phosphorylation of indicated molecules in single knock-down cells of EPHA2 or Ephrin-B1 alone or in a 1:1 mixture of both single knock-down cells. F, phosphorylation was calculated as fold change after normalizing with its total expression. Statistical analysis was done by paired-two tailed students t-test. *, **, ***, **** represents $p<0.05$, $p<0.01$, $p<0.001$ and $p<0.0001$, respectively.

Next, to check whether the interaction of Ephrin-B1 ligand with EPHA2 receptor leads to phosphorylation, we performed western-blotting experiment to identify their phosphorylation, on resides that are reported to be involved in biological activities (Fig. 2C-D). EPHA2 residues, Serine 897 (S897), Tyrosine 772 (Y772) and Tyrosine 594 (Y594) were showing hyper-phosphorylation in spheres. Similarly, Ephrin-B1 residues Y324/329 and Y317 were exhibiting hyper-phosphorylation in spheres. Contrary to these hyper-phosphorylations, Y588 of EPHA2 was showing reduced phosphorylations in spheres. As we expected, phosphorylation of EPHB2 at Y594/604 residue was showing reduced phosphorylation in spheres that imply that EPHB2 activation may not be important in spheres (Fig. 2C-D). So, our results show that when there is an enrichment of self-renewing population, there is an increased expression of Ephrin-B1 and EPHA2 leading to the increased phosphorylations of EPHA2 at S897, Y772, Y594 and Ephrin-B1 at Y324/329 and Y317. This increased phosphorylation could be due to the EPHA2-Ephrin-B1 interaction or it may be completely independent of it. To check that, we evaluated the change in the phosphorylation pattern when the ligand or receptor is depleted. Here, we checked how much of the receptor remain unphosphorylated when the ligand is absent and *vice versa*. None of the

phosphorylations of EPHA2 that were specifically upregulated in spheres (S897, Y594 and Y772) were reduced upon Ephrin-B1 knock-down, suggesting that these phosphorylations are independent of Ephrin-B1. At the same time, the phosphorylations of Ephrin-B1 at Y324/329 and Y317 reduced significantly upon EPHA2 knock-down (Fig. 2E-F). Thus, our results show that the interaction of Ephrin-B1 with EPHA2 leads to the phosphorylation of Ephrin-B1 at Y324/329 and Y317, while it is unclear whether it leads to the phosphorylation of any residues of EPHA2. Further, the enhanced phosphorylation of EPHA2 S897, Y594 and Y772 in the self-renewal enriched condition may depend on the *cis* or *trans* interaction of ligands other than Ephrin-B1. When Ephrin-B1 interacts with EPHA2, it could be in *cis* or *tran*s. To address that, we mixed equal proportion of EPHA2 knock-down cells and Ephrin-B1 knock-down cells to analyze the phosphorylations. In these mixed cells, EPHA2 and Ephrin-B1 interaction through *cis* manner will be reduced while *trans* interaction will be retained, since EPHA2 knock-down cells will express Ephrin-B1 and Ephrin-B1-depleted cells will have EPHA2. Mixing of the single knock-down cells failed to rescue the phosphorylation of both the residues of Ephrin-B1, implying that the interaction is a *cis* -interaction (Fig. 2E-F). Collectively, we show that Ephrin-B1 ligand interacts with EPHA2 receptor in spheres in a *cis*-manner, and leads to the phosphorylations of residues at Y324/329 and Y317 of Ephrin-B1 ligand, which may be contributing to the self-renewal ability of oral cancer stem cells (CSCs).

EPHA2/Ephrin-B1 signaling supports self-renewing cancer stem cell (CSC) pool in oral cancer cells

Since we anticipated that EPHA2/Ephrin-B1 signaling supports CSCs in oral cancer, we evaluated the change in CSC pool with the depletion of the receptor EPHA2 and the ligand Ephrin-B1. For this we used a CSC reporter ALDH1A1-DsRed2, which we have published earlier (Dharmapal *et al.*, 2021; Shanmugam *et al*, 2019). It was made by cloning the ALDH1A1 promoter gene upstream of DsRed2 in the DsRed2N1 plasmid (Fig. 3A). Lentiviral shRNA-mediated knock down was performed in the reporter cell lines (Fig. 3B-C). We analyzed ALDH1A1 positive population in the reporter cells with knock-down of EPHA2 or Ephrin-B1 through FACS analysis. FACS analysis indicated that knocked-down cells in the sphere condition had a higher reduction in ALDH1A1 positive population compared to monolayer (Fig. 3D-G). EPHA2-knock-down cells and Ephrin-B1-depleted cells exhibited a significant reduction in the ALDH1A1 positive CSC pool compared to control cells in the spheres as well as CSC enriched-monolayers (Fig. 3E-F). Further, we analyzed ALDH1A1-positive population in dual knock-down cells (both receptor and ligand), which showed superior reduction in ALDH1A1-positive CSC pool compared to single knock-down cells (Fig. 3G). It suggests that EPHA2/Ephrin-B1 signaling is important for the maintenance of ALDH1A1-positive CSC pool.

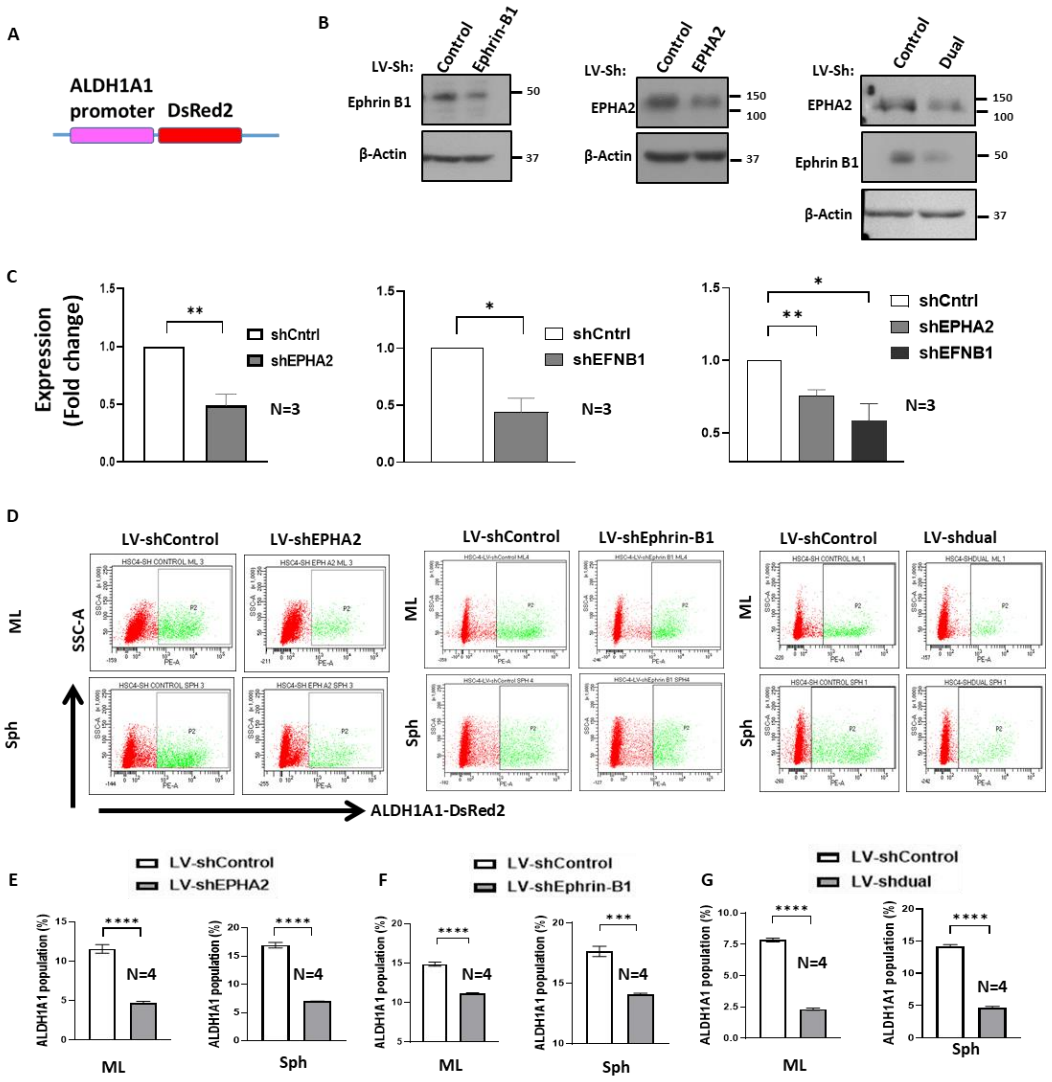

Figure 3. EPHA2/Ephrin-B1 signaling regulates self-renewing cancer stem cell pool in oral cancer cells. A, The vector construct of ALDH1A1-DsRed2 reporter. It was made by cloning the ALDH1A1 promoter gene upstream of DsRed2 in the DsRed2N1 plasmid. B, HSC-4 Reporter cells were made by transfecting this construct into oral cancer cell followed by FACS sorting of the ALDH1A1-DsRed2 positive cells. B, C, Western-blot to check the knock-down of the indicated molecules in HSC-4 ALDH1A1-DsRed2 cells, and the data represent fold change based on the control cells, after normalizing with β-Actin. D, E, FACS analysis to check ALDH1A1 population in knock-down cells in 3-Day old monolayer and spheres. E, Data indicates percentage of ALDH1A1 positive, CSC population plotted as mean ± SEM values from 4 replicates. Statistical analysis was done by paired-two tailed students t-test. *, **, ***, **** represents $p<0.05$, $p<0.01$, $p<0.001$ and $p<0.0001$ respectively.

To further explore the functional role of EPHA2/Ephrin-B1 signaling, we used single knock-down of either receptor or ligand and dual knock-down of both for functional assays (Fig. S4A-B). We performed more robust self-renewal functional assays, like extreme limiting dilution assay (Hu & Smyth, 2009). First, we did an *in vitro* serial dilution sphere formation assay to evaluate the effect of the knock-down of the ligand and the receptor (Fig. 4A). The depletion of EPHA2 significantly reduced the CSC frequency in oral cancer cells (4.5-fold reduction in RCB1015 and 2.5-fold reduction in HSC-4 cells (Fig 4B-C Fig. S4C). Similarly, knock-down of Ephrin-B1 caused 2.5-fold reduction in the CSC pool (Fig. 4B-C). Although we observed a significant reduction in the CSC frequency, the single knock-down did not substantially change the size of the spheres or the number of spheres formed in each dilution (Fig 4A, Fig. S4C-D). Interestingly, the dual knock-down of EPHA2 and Ephrin-B1 drastically reduced the CSC frequency (6-fold reduction), sphere size and number of spheres formed in each dilution (Fig 4A-C, Fig. S4D-E). So, our observations show that abolishing both ligand and receptor in the same cell, disrupting the EPHA2/Ephrin-B1 signaling, drastically depletes CSCs. Then, to analyze whether *in vitro* studies are concordant with *in vivo* scenario, we did an *in vivo* serial dilution xenograft assay. Similar to *in vitro* results, CSC frequency was significantly reduced upon the depletion of EPHA2 (Fig. 4D, Fig S5A) or Ephrin-B1 (Fig. 4E, S5B). In agreement to this, the expression of self-renewal molecules like SOX2 and OCT4A showed a reduction in the ligand or receptor knocked-down tumors (Fig. S5C-D). Taken together, all these results show that abrogation of EPHA2/Ephrin-B1 signaling abolishes CSCs *in vitro* and *in vivo*.

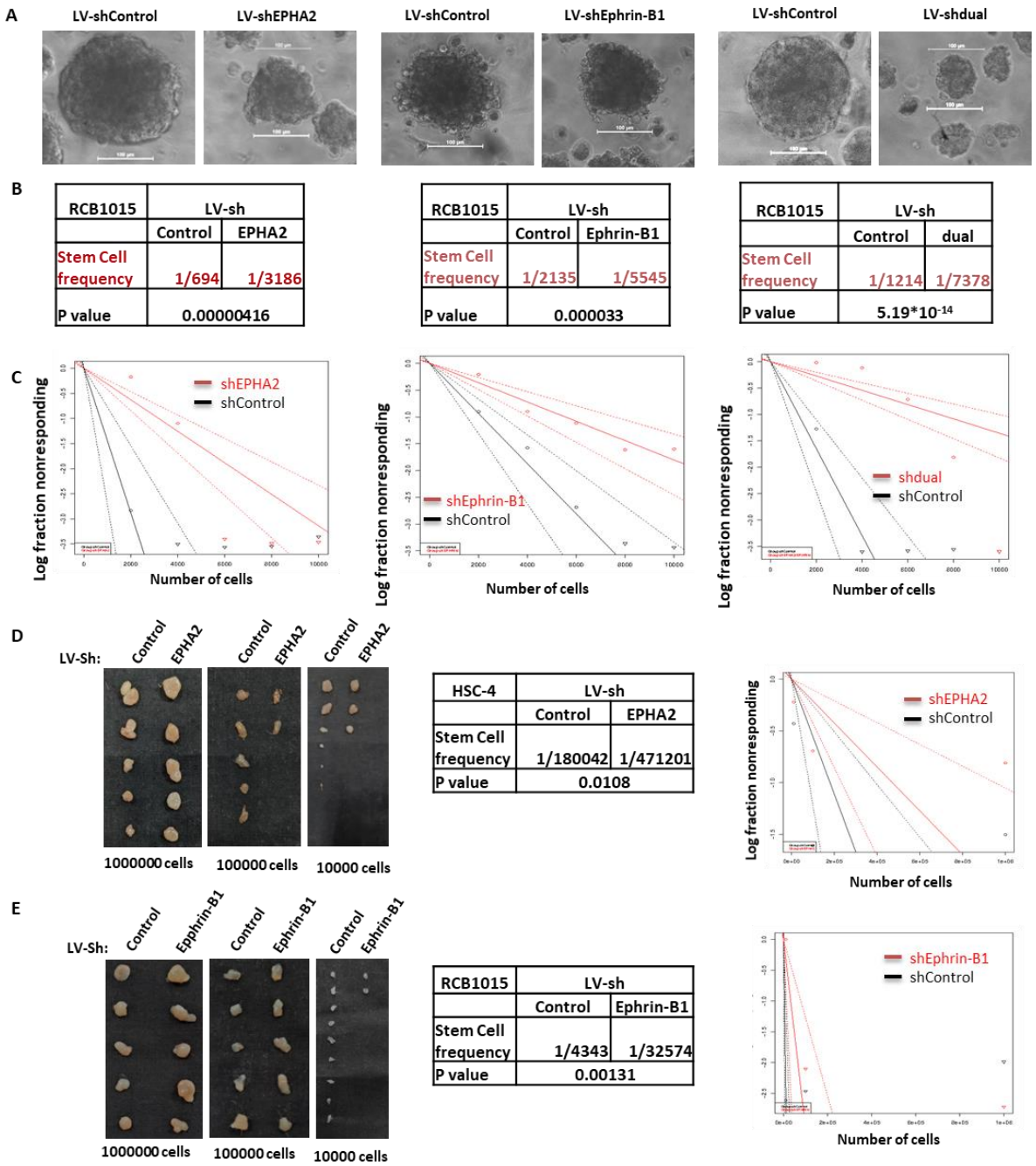

Figure 4. Abrogation of EPHA2/Ephrin-B1 signaling depletes self-renewing cancer stem cell pool in oral cancer cells. A, RCB1015 cells with knock-down of EPHA2, Ephrin-B1 or both molecules were seeded at different serial dilutions in Poly-HEMA coated 96-well plate and were grown as spheres for 6 days. Image showed size of the spheres formed in the dilution of 10,000 cells/well. The scale bar represented 100µm. B Cancer stem cell frequency calculated by ELDA C, Graph represented log fraction plot obtained from ELDA analysis, and slope of it represented cancer stem cell frequency. D, E, For serial dilution xenograft formation assay, cells were serially

diluted to 10^6, 10^5 and 10^4 cells. These cells were injected subcutaneously on the flanks of the NSG mice. First figure in D represented the image of tumors collected after 14 days from 10^6, and 10^5 dilutions while tumors were collected after 40 days from 10^4 dilution. First figure in E represented the image of tumors collected after 17 days from all the dilutions. Tables in D and E showed cancer stem cell frequency, and graphs represented log fraction plot obtained from ELDA analysis.

Abrogation of EPHA2/Ephrin-B1 signaling increases the overall survival in mouse model of oral cancer

Since CSCs exhibiting self-renewal ability is shown to critically regulate tumor properties, deciding prognosis of the diseases, we evaluated the role of this signaling pathway in the overall survival using orthotopic mouse model of oral cancer. Even though mice injected with EPHA2 or Ephrin-B1 knocked-down cells exhibited a delayed tumor progression, dual knock-down cells injected mice displayed a drastic retardation in the tumor progression (Fig. 5A-B).

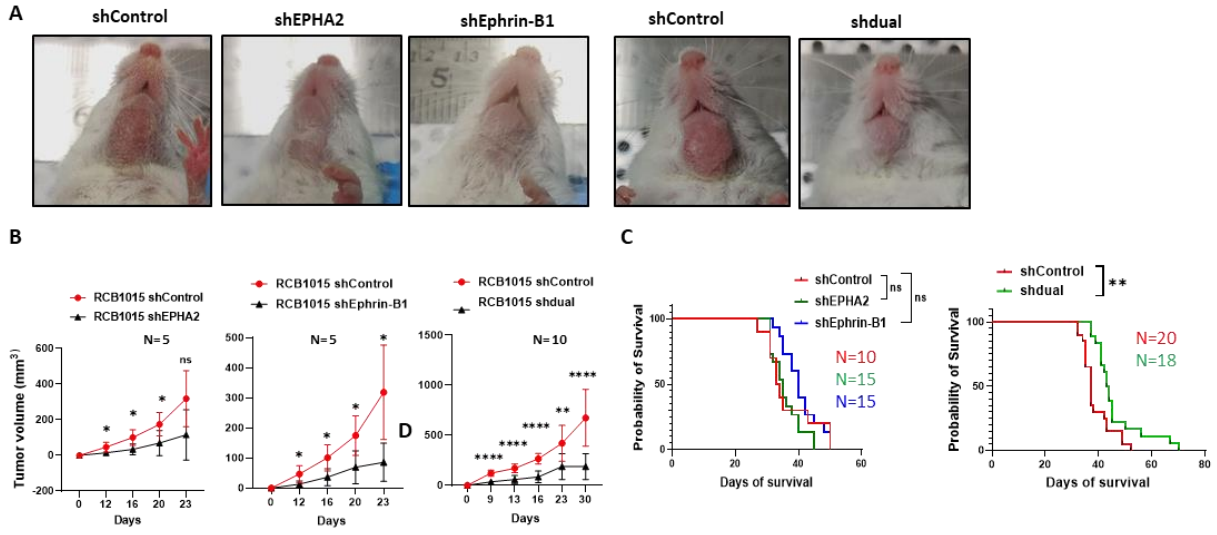

Figure 5. Role EPHA2/Ephrin-B1 signaling in the prognosis of oral cancer using mouse model. overall survival analysis was performed using orthotopic floor of the mouth mice models. 0.5×10^6 cells were injected to the floor of the mouth region superficial to the mylohyoid muscle. RCB1015 shControl, shEPHA2 and shEphrin-B1 cells were injected to SCID mice while RCB1015 shControl and shDual cells were injected to NSG mice. A, Representative image of

mice with tumor after 24 days. B, We measured tumor size using digital Vernier caliper in regular interval and plotted tumor volume against number of Days. Tumor volume was calculated using the formula (Height*Height*width)/2. Statistical analysis was done by paired-two tailed students t-test. *, **, **** represents $p<0.05$, $p<0.01$, $p<0.001$ and $p<0.0001$, respectively. C, Kaplan-Meier survival analysis was performed using GraphPad Prism to check overall survival. ** represents $p<0.01$.

Then, we used Kaplan-Meier analysis to study the prognosis with respect to overall survival. Though there was a trend in Ephrin-B1 depleted group to show improved survival, with single knock-down of either receptor or ligand was incapable to significantly alter the overall survival of the mice, while the mice injected with dual knocked-down cells showed a significant improvement in overall survival (Fig. 5C). To summarize, the loss of EPHA2 and Ephrin-B1 in the same cell, reducing their cis-interaction and signaling, reduces the tumor progression and improves the prognosis by enhancing overall survival.

EPHA2/Ephrin-B1 signaling critically regulates the prognosis of oral cancer

Our mouse model data showing the role of EPHA2/Ephrin-B1 signaling regulating overall survival prompted us to explore the role of this signaling on the overall survival of oral cancer patients. First, we checked whether there is any difference in the expression of the ligand and the receptors we identified in the study, in oral cancer compared to the normal tissues, using TCGA datasets. The transcript levels of Ephrin-B1 (*EFNB1*) and EPHB2 (*EPHB2*) was significantly upregulated in the malignant tissues, compared to its normal counterpart. Though there was a trend of upregulation, the levels of EPHA2 (*EPHA2*) did not significantly change in the two conditions (Fig. S6A). Yet, when we analyzed the correlation of Ephrin-B1 with the receptors by hierarchical clustering heat map analysis using TCGA data, the correlation with *EPHA2* was more than with *EPHB2* receptor (Fig. S6B-C). Then, we checked the protein expression of EPHA2, EPHB2 and

Ephrin-B1 in relation to ALDH1A1 in the primary oral cancer samples to check the dependency of this signaling with CSCs, as ALDH1A1 is a reported CSC marker for oral cancer.

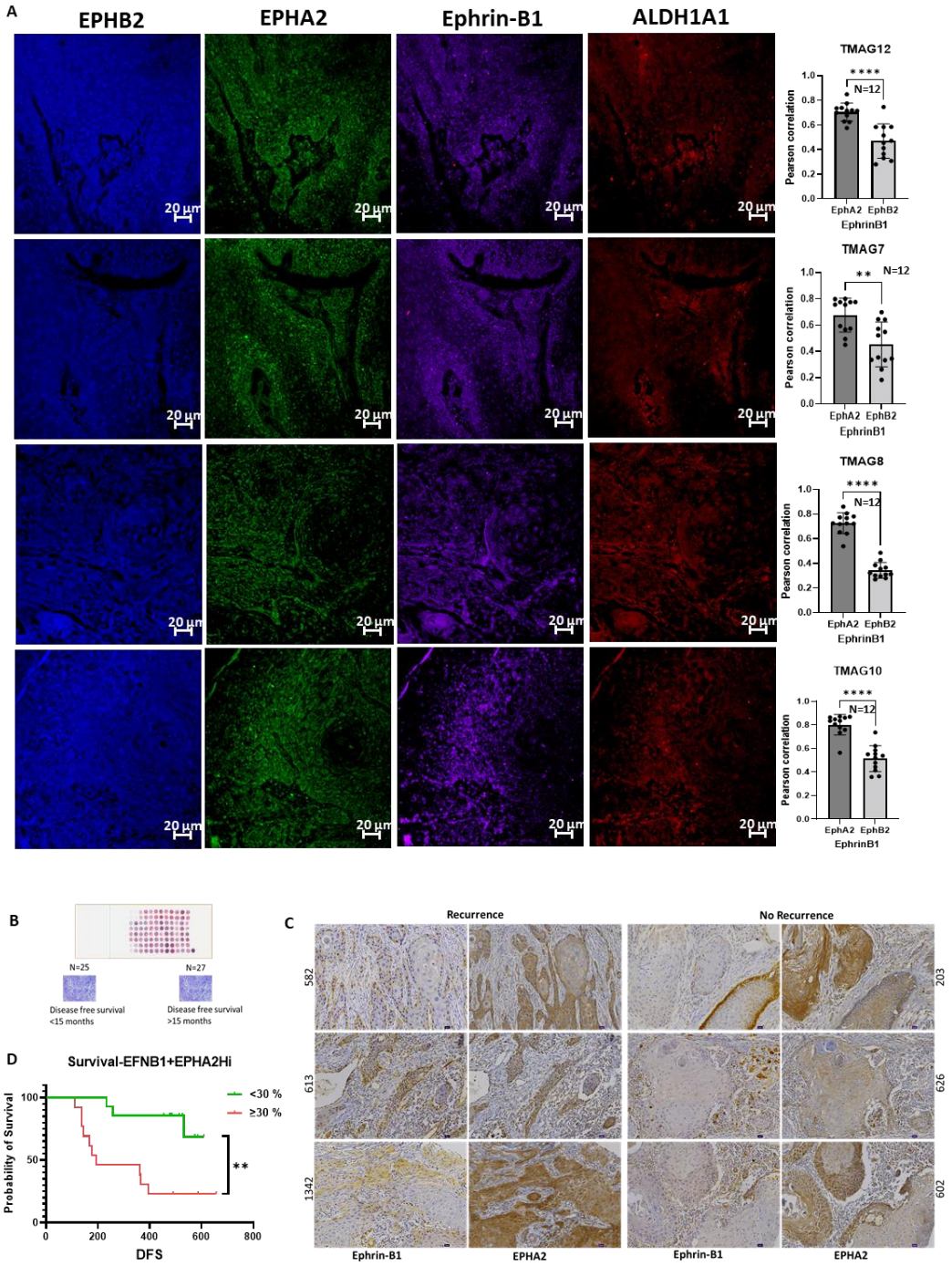

Figure 6. Role EPHA2/Ephrin-B1 signaling in the prognosis of oral cancer patients. A, OSCC patient samples were co-stained for the indicated molecules using tagged primary antibodies, EPHB2-Alexa 405, EPHA2-Alexa 488, EphrinB1-Alexa 680 and ALDH1A1-Alexa 568. From multiple images at 40X, we chose 12 ROI to check the co-localization using Pearson correlation analysis. **, **** represents $p<0.01$ and $p<0.0001$, respectively. B, OSCC patients were categorized as recurrent and non-recurrent groups where patients with disease free survival of less than 15 months were considered as recurrent while patients with disease free survival for more than 15 months were considered as non-recurrent group. C, Tissue array IHC was performed on serial sections. D, Tumor bundles with high expression of EPHA2 ($EPHA2^{Hi}$) and positivity for Ephrin-B1 were scored. Then, percentage of tumor bundles with $EPHA2^{Hi}$ and Ephrin-$B1^{+}$ co-expression was calculated. The patients were grouped as two where one group had less than 30% of tumor bundles with co-expression of Ephrin-B1 and higher expression of EPHA2 while second group had more than 30% of co-expression of both the molecules. Kaplan-Meier survival graph for Disease free survival was plotted between those two groups. ** represents $p<0.01$.

An immunohistochemical analysis of oral cancer samples co-stained with these four molecules revealed that the expression of EPHA2 receptor and Ephrin-B1 ligand were confined to certain clusters, while the expression of EPHB2 was uniform throughout the section (Fig. 6A). More specifically, some regions of the tissue sections had high expression of both EPHA2 and Ephrin-B1, which showed a better co-localization than the Ephrin-B1-EPHB2 co-localization, as revealed by Pearson correlation analysis (Fig. 6A). So, in accordance with our *in vitro* cell line data, the primary oral cancer sample data also suggested the EPHA2-Ephrin-B1 co-localization leading to signaling, within the region positive for ALDH1A1, defining the CSC niches of the tumors. The expressions of both Ephrin-B1 and EPHA2 were observed in the same cell, suggesting the *cis*-interaction, which we deducted from our biochemical analysis. Here, we observed that ALDH1A1 population is restricted to the region where EPHA2-Ephrin-B1 co-localization is seen (Fig. 6A), supporting the notion that the interaction of EPHA2 and Ephrin-B1 in the same cell, leading to EPHA2/Ephrin-B1 signaling, supports self-renewing CSCs in oral cancer.

Then we checked the correlation of the expression of the ligand and the receptors to the overall survival. Although patients with the high expression of either one of the ligand or receptor

did not show any difference in the prognosis, the high expression of both the receptor and ligand exhibited poor overall survival compared to the group showing the low expression of both (Fig. S6D-E). Since the prognosis of oral cancer is dependent on the recurrence of the disease, we studied that aspect also. We segregated oral cancer patients into recurrent and non-recurrent category, patients with disease free survival lesser than 15 months were considered as recurrent group while more than 15 months were non-recurrent group (Fig. 6B). Further, tissue microarray immunohistochemical (IHC) analysis was performed on recurrent and non-recurrent OSCC samples using EPHA2, and Ephrin-B1 antibodies (Fig. 6C). Irrespective of the recurrence status, the expressions of the receptors were high in all tumor tissues. The Ephrin-B1 expression was limited to the outer layers of tumor bundles than the core of the bundle. Then, tumor bundles in the samples were scored based on the co-localization of high expression of EPHA2 ($EPHA2^{Hi}$) and Ephrin-B1 positivity in the sample. Then, percentage of tumor bundles with co-localization $EPHA2^{Hi}$ and Ephrin-$B1^{+}$ in each sample were calculated. The co-expression of the ligand Ephrin-B1 and the receptor EPHA2 offers the chance of their interaction to modulate the signaling. Recurrent group showed higher percentage of tumor bundles with co-localization of $EPHA2^{Hi}$ and Ephrin-$B1^{+}$ (Fig. S7A). Kaplan-Meier survival analysis showed that the disease free survival of patients with less than 30% of tumor bundles with co-expression of Ephrin-B1 and higher expression of EPHA2 is more compared to patients with high co-expression of both the molecules (Fig. 6D). Thus, our IHC analysis of the tissue microarray reinforced our hypothesis that the interaction of Ephrin-B1 with EPHA2, in a *cis*-manner, critically regulates the chance of recurrence of oral cancer.

Discussion

Recurrence is a major driving factor for poor prognosis in many cancers including lung, breast, bladder and oral cancer (Jain *et al*, 2024; Jeong *et al*, 2022; Lee *et al*, 2023; Wang *et al*, 2013; Zhao *et al*, 2022). Among these cancers, oral cancer is a major burden in Asian countries, especially in India. Recurrence occurring as loco-regional or distant metastasis leads to the death of one out of two oral cancer patients (Davaatsend *et al*, 2024; Wang *et al.*, 2013). The recurrence depends more on the self-renewal property of cancer cells than the stage and grade of the cancer (Banki & Moosavi, 2023; Mirshahidi *et al*, 2024). So, it is important to target these self-renewing cancer stem cells (CSCs) for which we need to identify surface molecules and pathways that regulate them. In self-renewal enriched spheres, we identified the enrichment of the surface expression of Ephrin-B1 ligand, which is a mediator of Eph-Ephrin signaling. Moreover, a phosphoproteomic analysis identified Eph-Ephrin signaling as one of the differentially regulated pathways in spheres. The phosphorylation pattern and the enrichment of the ligand and receptors in the sphere condition that enriches CSCs suggested a possibility of Ephrin-B1-mediated EPHA2 signaling, supporting CSCs (Fig 1). Though Ephrin-B1 is established to regulate normal stem cells, its role in the regulation of CSCs are less investigated except the first report from our lab, which showed that surface expression of Ephrin-B1 is essential for the support of CSCs in oral cancer (Dharmapal *et al.*, 2021). Ephrin-B1 is however reported to be overexpressed in many cancers, including oral cancer (Castellvi *et al*, 2006; Dharmapal *et al.*, 2021; Sawai *et al*, 2003). Also, the over-expression is correlated to angiogenesis, aggressiveness of tumor and recurrence (Castellvi *et al.*, 2006). Even though EPHB2 receptor is reported as the regular binding partner for Ephrin-B1 in different contexts, as in stem cell-homeostasis of intestinal crypt as well as cance,r by regulating invasion, metastasis and immunomodulation (Batlle *et al.*, 2002; Hu *et al*, 2024; Liu *et*

al, 2022). But, whether the same receptor molecule interacts with Ephrin-B1 in the CSC context is unknown. Since our findings suggested that Ephrin-B1 and its signaling is important in regulating self-renewal of cancer cells, it is important to identify the receptor molecule for Ephrin-B1 in the regulation of self-renewal.

The receptor molecules obtained from our phospho-proteomic analysis, EPHB2 and EPHA2, are reported to be overexpressed in HNSCC and oral cancer, respectively (Bai *et al.*, 2024; Phan *et al*, 2020). Higher expression of these receptor molecules in cancer patients lead to poor prognosis in patients, implying that they have a role in the progression of cancer (Bai *et al.*, 2024; Zhao *et al*, 2017). As we have shown, the expression of EPHB2 transcripts and its protein are high in the oral cancer, suggesting its role in the regulation of malignant properties (Fig. S6A, Fig. 6C). Though our results did not support the role of EPHB2 in the self-renewal in oral cancer, it is reported to enrich CSCs to impart sorafenib resistance in hepatocellular carcinoma, by the up-regulation of WNT-β-catenin pathway (Leung *et al*, 2021). Despite that, its expression is a predictive marker for relapse-free survival in colorectal cancer, gastric cancer and breast cancer, disapproving its role in the positive regulation of CSCs and recurrence in all malignancies (Ebrahim *et al*, 2021; Jang *et al*, 2018; Kim *et al*, 2022). Even if EPHB2 does not regulate self-renewal property and CSCs, the signaling mediated by the receptor might have critical roles in the regulation of other malignant properties. The EPHB-Ephrin-B interaction is reported to induce fibroblast remodeling to generate cancer associated fibroblasts (CAFs), and increase invasion and metastasis (Kakarla *et al*, 2022).

As we consider the second receptor EPHA2, it is demonstrated to regulate CSCs of many cancers including oral cancer, which aligns with our findings (Bai *et al.*, 2024; Binda *et al.*, 2012;

Song *et al.*, 2014). Additionally, our study proposes the role of EPHA2 receptor in regulating recurrence where we observed the co-expression of EPHA2 receptor and Ephrin-B1 ligand correlates with recurrence in oral cancer patients (Fig 6B-C, Fig. S7A). Since we observed that there is enhanced surface expression of Ephrin-B1 ligand and EPHA2 receptor when there is an induction of self-renewal (Fig 1), we investigated whether they interact to initiate signaling. Our co-immunoprecipitation experiments showed that the co-expression leads to the interaction of EPHA2 and Ephrin-B1 in the self-renewal enriched sphere condition. A series of western blot analyses confirmed that this interaction leads to the specific phosphorylation of Y317 and Y324/329 residues of Ephrin-B1 (Fig. 2C-F). Though the functional significance of these phosphorylations of Ephrin-B1 is not known, it was identified as a phosphorylation induced by soluble EphB2 (Kalo *et al*, 2001). Apart from the enhanced phosphorylations of Ephrin-B1, we detected some EPHA2 phosphorylations that are specifically increased in the sphere condition, even though they were independent of the interaction with Ephrin-B1 (Fig. 2C-F). In accordance with our results, EPHA2 S897 is a residue that is reported to regulate CSCs (Li *et al.*, 2019). This phosphorylation is shown to be regulated by kinases that are not included in EPH/Ephrin family, like AKT (Gehring & Pasquale, 2020; Miao *et al*, 2009), clarifying why it did not alter with the loss of Ephrin-B1. The Y772 phosphorylation is shown to be a ligand-independent phosphorylation, promoting proliferation and anchorage independent growth (Xiang *et al*, 2020), explaining its relevance in anchorage independent sphere culture, possibly supporting CSCs. Another residue that was showing hyperphosphorylation was Y594, a ligand dependent phosphorylation, possibly interacting with the kinase domain (Lechtenberg *et al*, 2021). Even though EPHA2 S897, Y772 and Y594 are not phosphorylated by Ephrin-B1, they might be regulated by interactions with other ligands, in *cis* or *trans*, to support CSCs.

Since our focus was on Ephrin-B1, we further explored the signaling initiated when it interacts with EPHA2. It is well established that Eph receptors and Ephrin ligands can interact in *trans* or *cis*, where conventionally it is believed that the *trans*-interaction leads to signaling events, and the *cis*-interaction blocks the *trans*-interaction (Falivelli *et al*, 2013; Yin *et al*, 2004). As the co-culture of single knock-down of ligand or receptor retains the *trans* interaction while blocking the *cis* interaction, we performed our western blot analysis of the phosphoforms in that condition. Here, we showed that the *trans* interaction of the ligand and the receptor does not compensate the loss of phosphorylation, suggesting that the *cis*-interaction of Ephrin-B1 with EPHA2 leads to Ephrin-B1 phosphorylation (Fig. 2E-F). To summarize, our results show that in a self-renewal enriching condition, there is enhanced co-expression of EPHA2 and Ephrin-B1, leading to the higher chance of their interaction and more number of molecules getting phosphorylated. Moreover, the enhanced molecules may interact with possible ligand in *cis* or *trans*, and the *cis*-interaction of Ephrin-B1 with EPHA2 is one of the important signaling event in the sphere condition.

Though our results indicate that the EphrinB1-EPHA2 interaction is important for the self-renewal, we had to confirm that this pathway is important for the self-renewing population in cancer cells, and it regulates recurrence in patients. We used a functional assay to check the CSC frequency by extreme limiting dilution assay (ELDA), which showed a pronounced reduction in CSC frequency, both *in vitro* and *in vivo*, in dual knock-down cells compared to single knock-down cells, where the ligand receptor interaction is blocked (Fig. 4, Fig. S4). The same result was reproduced with an ALDH1A1-DsRed2 CSC reporter cells (Fig. 3). Both the results emphasize the importance of both EPHA2 and Ephrin-B1, and also the signaling initiated by their interaction. Next, to examine whether this regulation of CSCs translate to the prognosis, we checked the overall

survival of OSCC patients using Kaplan-Meier analysis correlating to the signaling. Our observation that the patients with higher expression of both receptor and ligand had decreased overall survival time compared to patients having low expression of both, underscore the significance of this interaction and the EphrinB1-EPHA2 signaling (Fig. S6D-E). Further, this observation was validated using orthotopic floor of the mouth mice models injected with single knock-down or dual knock-down cells (Fig. 5). The pattern of expression of EPHA2 and Ephrin-B1 in the OSCC samples suggest that the *cis*-interaction is clearly enhanced in malignant tissues of patients, who showed recurrence within 15 months (Fig. 6B-C).

To conclude, in the current study we demonstrate the importance of Ephrin-B1 in the regulation of self-renewal ability of oral cancer cells, which in turn regulates the chance of recurrence of the disease, for the first time. Also, we show that cis-interaction can also lead to certain signaling events, which are critical for the maintenance of self-renewal ability in cancer cells. As many of the studies have shown that EphB-Ephrin-B interaction is crucial for the sustenance of stem cells in normal stem cell contexts, this EPHA2/Ephrin-B1 interaction, that manifest in tumor microenvironment might serve as an attractive target for therapy, which needs further validation.

Materials and Methods

Ethics statement

For the studies involving fresh oral cancer samples, the tumor tissues were collected after getting informed consent from the patients from Regional Cancer Centre, Thiruvananthapuram. The protocol was approved by the the Institute Human Ethical Committee of Rajiv Gandhi Centre for Biotechnology (IHEC/1/2011/04), and Regional Cancer Centre, Thiruvananthapuram

(HEC/24/2011). Paraffin embedded tissue blocks for making the tissue microarray (TMA) were collected from the archives of Cochin Cancer Research Centre, Cochin, and the preparation of TMA, IHC staining, scoring and imaging were done at St. Johns Research Institute. The protocol was approved by Institute Human ethical committee of all the respective study centers (IEC/150/2023, IHEC/1112022_Exl11). All the animal experiments were conducted adhering to the ARRIVE guidelines, and as per the approved guidelines of the Institute Animal Ethics Committee (IAEC/874/TM/2002, IAEC/875/TM/2002 and IAEC/894/TM/2002) which is under the Committee for the Control and Supervision of Experiments on Animals (CCSEA), Govt. of India. The recombinant DNA works were reviewed and approved by the Institutional Bio-safety Committee (71/IBSC/TTM/2022, 72/IBSC/TTM/2022).

Antibodies

The antibodies, p-Raf-1, p38 MAPK (MAPK 1/3), TUBB, TUBB2A, TUBA1C, TUBB4B, ERO1L, TUBB3, NDRG1, GAL3, FSCN, GAL1, DSG3, ALDH1A1, Ephrin-B1, EPHA2, EPHB2 and β-Actin were purchased from Santa Cruz Biotechnology, Inc. The other antibodies used were either from Cell Signaling Technology [p-Bad, p-Akt, p-STAT3, pp38 MAPK, SOX-2, OCT4A, EPHA2, Ephrin-B1, pEPHA2 (S897), pEPHA2 (Y772), pEPHA2 (Y594), pEPHA2 (Y588), pEphrin-B (Y324/329)] or Invitrogen, Thermo Fischer Scientific-US [pEPHB1/2 (Y594/604), pEphrin-B1 (Y317)]. Peroxidase conjugated AffiniPure Donkey Anti Mouse, AffiniPure Donkey Anti Goat, and AffiniPure Donkey Anti-Rabbit Secondary Antibodies) were purchased from Jakson ImmunoResearch Laboratories Inc. Peroxidase conjugated Veriblot for Co-IP experiments was purchased from Abcam. We used Donkey Anti-Goat Alexa Fluor-568, Donkey Anti-Mouse Alexa Fluor-568, Donkey Anti-Rabbit Alexa Fluor-568, and Donkey Anti-Goat Alexa Fluor-680

(Invitrogen, Thermo Fischer Scientific-US) for immunofluorescence and immunohistochemistry experiments.

Cell lines

The cell lines RCB1015, RCB1017, HSC-4, and HSC-3 were obtained from Riken Cell Bank, Japan. All these cell lines were maintained in Dulbecco's Modified Eagle's Media with 10% FBS. HSC-4 and HSC-3 cells with stable expression of ALDH1A1-DsRed2 were maintained in 20µg/mL geneticin-containing medium. Cells stably infected with LV-shRNA particles were maintained in 100ng/mL puromycin-containing medium.

Monolayer and sphere culture

Sphere cells were grown using Opti-MEM (1X) Reduced serum (Invitrogen) medium supplemented with 1X N-2, 20µg/ml EGF and bFGF, and 1X Insulin-Transferrin-Selenium (sphere medium). Monolayer culture was maintained in DMEM in the presence of 10% FBS.

Soft agar colony formation assay

The assay was performed using both monolayer and sphere culture. 5000 cells were seeded for the analysis. After 21 days, the colonies were counted at 10X magnification, and number of colonies/10 fields were plotted.

RNA isolation and RT-PCR (Reverse transcription PCR)

We used the RNeasy mini kit (Qiagen) for RNA isolation from the oral cancer cells. Then, the isolated RNA was quantified using NanoDrop for cDNA preparation. A reaction mix containing RNA (3.5 µg), 5X RT buffer (1X), DNTP (0.1mM), random hexamer primer (10µM), reverse transcriptase enzyme, and RiboLock was used to reverse transcribe total RNA to cDNA. Further,

we performed PCR to check gene expression using gene-specific primers and separated DNA bands using agarose gel for electrophoresis. Then, bands were visualized in Gel Doc EZ imager (Biorad). Reagents for reverse transcription and PCR reaction were purchased from Invitrogen.

SILAC labeling

For SILAC labeling, HSC-4 monolayer cells were grown in arginine and lysine-free DMEM (Invitrogen) supplemented with heavy arginine and lysine ($^{13}C_6$ Arg/$^{13}C_6$Lys;+6Da and +4 Da). SILAC-labeled cells were grown as monolayer cultures while HSC-4 sphere cells were maintained in sphere medium as mentioned above.

Membrane preparation for LC-MS/MS analysis

The sample preparation and proteomic analysis were done as reported before (Kristiansen *et al*, 2008). The cell lysis was done in a high salt buffer (2M NaCl, 10mM HEPES, pH 7.5, 1mM EDTA, pH 8.0) using a polytron tissue homogenizer. The supernatant collected after the centrifugation of the lysate at 250,000 g for 45 min at 4°C was discarded, and the pellet was re-suspended in 0.1 M Na2CO3, pH 11 using a polytron homogenizer, and left on ice for 45 min. The high salt lysis and Na2CO3 wash were repeated an additional two times and the pellet containing the membranous material was used for LC-MS/MS analysis using hybrid LTQ–OrbitrapVelos ETD.

Cell lysis, Trypsin digestion, phosphopeptide enrichment for LC-MS/MS analysis

The sample preparation was carried out as described before (Harsha *et al*, 2013). Briefly, the monolayer cells were scraped in PBS and centrifuged to get the cell pellet. Sphere cells were pelleted in the sphere medium and then washed with PBS. Cell pellets were lysed in 9M urea lysis

buffer by sonication. The lysates were centrifuged at 12,000 g for 15 min and cleared supernatant was collected. The protein concentration of the lysates was estimated using the BCA method and 3 mg protein from both monolayer and sphere cultures was pooled. Proteins were reduced using 5mM dithiothreitol at 56°C for 45 min. Proteins were further alkylated using iodoacetamide at a final concentration of 10mM and incubated the lysate at room temperature in the dark for 30 min. Lysates were diluted to obtain a final urea concentration of <2 M using HEPES buffer. Sequencing grade trypsin was added to achieve enzyme to substrate ratio of 1:20 (w/w). Trypsin digestion was carried out overnight at 37°C. Peptide digest was acidified using trifluoroacetic acid (TFA) at a final concentration of 1%. The acidified peptide digest was centrifuged at 4,500 g for 15 min and the supernatant was desalted using a C18 Sep-Pak cartridge. The desalted peptide digest was frozen and lyophilized for 48 hrs. The lyophilized peptides were reconstituted in 7mM Triethylammonium bicarbonate buffer (pH 9). Peptides were fractionated into 12 fractions using basic reverse phase chromatography. The samples were dried at 4°C and reconstituted in 100 µl of 5% 2, 5-dihydroxybenzoic acid (DHB). TiO_2 beads (GL Sciences, Inc., Japan Catalogue # 5020-75010) were washed in 5% DHB solution for 15 min. For each fraction, 2 µl of beads was added to achieve the TiO_2: peptide ratio of 1:1 and incubated on a rotator for 15 min at room temperature. The vials were centrifuged at 1,500 g for1 min and supernatant with unbound peptides was discarded. The beads were reconstituted in 5% DHB solution and loaded on to C8 Stage Tip. The beads were washed twice with 100 µl of 80% acetonitrile with 1% TFA. The phosphopeptides were eluted from TiO_2 beads using 30 µl of 2% NH_4OH solution, pH 10.5 (prepared by dissolving 20 µl of NH_4OH in 1 ml of 40% ACN) into collection tubes containing 20 µl of 0.1% TFA. Then, the phosphopeptides were analyzed using hybrid LTQ–OrbitrapVelos ETD.

LC-MS/MS analysis

Samples were analyzed on a hybrid LTQ–Orbitrap Velos ETD (ThermoScientific, Bremen, Germany) mass spectrometer equipped with a nanoelectrospray ion source interfaced with an Easy nano-LC (Thermo Scientific, Bremen, Germany) for sample delivery. The samples were loaded on to a 2 cm trap column (75 µm ID; Magic C 18 AQ, 5µm, 100 Å, Michrom Bioresources Inc.) using 1% formic acid with a flow rate of 3 µl/min and further resolved on a 15 cm analytical column (75 µm ID; Magic C 18 AQ, 3µm, 100 Å, Michrom Bioresources Inc.) using a 100-minute gradient from 5% to 30% acetonitrile in 0.1% formic acid with a flow rate of 350 nl/min before introducing into the mass spectrometer. The spray voltage was set to 2.2 kV while the capillary temperature was set to 250°C. The MS instrument was operated in data-dependent acquisition mode. A survey scan from m/z 350–1,700 was acquired in the Orbitrap with resolution 60,000 with a maximum AGC target value of 1,000,000 ions. The fifteen most intense peptide ions with charge states ≥2 were sequentially isolated to a target value of 50,000 ions and fragmented in the higher-energy collisional dissociation (HCD) cell using 39% normalized collision energy. The maximum ion injection time for MS and MS/MS were set to 100 ms and 200 ms, respectively. Fragment ion spectra were detected in the Orbitrap mass analyzer with a resolution of 7,500. For all measurements with the Orbitrap detector, a lock-mass ion from ambient air (m/z 445.120025) was used for internal calibration.

Data analysis

The mass spectrometry-derived data were searched against the Human RefSeq database (Version 52) using SEQUEST and Mascot search algorithms through Proteome Discoverer software (Version 1.4.1.14) (Thermo Scientific, Bremen, Germany). The protease was specified as

trypsin and a maximum of 1 missed cleavage was allowed. Carbamidomethylation of cysteine was set as a fixed modification while oxidation of methionine, phosphorylation at serine, threonine, and tyrosine, and SILAC-labelling ($^{13}C_6$) at lysine and arginine were set as variable modifications. MS and MS/MS mass tolerances were set to 10 ppm and 0.05 Da, respectively. Peptide identification was based on a 1% false discovery rate calculated using target-decoy database searches. The SILAC ratio for each peptide-spectrum match (PSM) was calculated by the quantitation node and the peptides with ratios greater than two-fold were considered as differentially regulated and were considered for further bioinformatics analysis.

Bioinformatic analysis

The phosphoproteins identified <0.5 fold and >2 fold were considered as regulated molecules. The two biological replicates were analyzed separately for pathway enrichment using Genespring Version B13.0. A single Experiment Analysis with 700 source pathways identified the regulated pathways and the molecules regulated in each pathway. All the pathways with $p<0.05$ were considered as significantly regulated. A Venn diagram of the significantly regulated pathways from the biological replicates identified consistently regulated pathways. The list of regulated molecules in each pathway was used to study the overlap of pathways.

Western blotting

Cell lysate was prepared using lysis buffer (0.15 M Sodium chloride, 0.025M Tris, 0.001 M EDTA, 0.5% (v/v) NP40, 0.5% (v/v) Triton X 100, 5% glycerol (v/v), 1× protease inhibitor, pH 7.4). The tumor lysate was prepared using RIPA buffer (150mM NaCl, 1% (v/v) NP40, 0.5% (v/v) Sodium deoxycholate, 1% (v/v) SDS, 50mM Sodium orthovanadate, 10mM Sodium Fluoride). The proteins were resolved using SDS-PAGE followed by the wet-transfer of proteins to

nitrocellulose membrane. After a 10 minutes wash with TBST (500 mM Tris, 1.5M NaCl, 0.15% (v/v) Tween 20), the membrane was blocked using 3% BSA or 10% milk for 1 hour. Then, the membrane was incubated with primary antibody overnight. The next day, membrane was washed thrice with TBST to remove unbound primary antibody and incubated in secondary antibody for 1 hour at room temperature. After three times washing with TBST, the membrane was developed using ECL reagent (Biorad).

Immunofluorescence (IF)/ Immunohistochemistry (IHC)

Oral cancer cells were grown as monolayer and spheres for 3 days in confocal dishes. Then, the cells were washed with PBS and fixed using 4% paraformaldehyde (PFA) for 10 minutes. The cells were permeabilized and blocked with 2% fetal bovine serum (FBS) in PBS for surface molecules or with 2% FBS in PBST which contained 0.3% (v/v) Triton X-100 for intra-cellular molecules for 0.5-1 hour. After removing blocking, cells were incubated in primary antibody overnight. The next day, cells were washed and incubated with the secondary antibody for 1 hour. Then, nuclei were stained using DAPI and washed with PBS to remove excess antibody and DAPI. Further, cells were mounted with antifade (Invitrogen) and imaged with confocal microscope Olympus FV3000 or Nikon A1R LSCM.

Oral cancer patient samples were collected and fixed with 4% PFA for 1 day followed by storage in 30% sucrose solution. Then, 5µm sections were taken in a LeicaCM1850UV Cryostat. The antigen unmasking was done using 0.01M Citrate buffer. The IHC staining protocol was similar to IF that used for cultured cells.

Fluorescence Activated Cell Sorting (FACS):

Cells were trypsinized and resuspended the pellet in DMEM with 10% FBS. Then, the cells were kept inside a CO2 incubator for 1 hour for re-expression. Then, cells were pelleted and fixed with 4% PFA for 10 minutes. After one PBS wash, cells were incubated with Alexa fluor-488 tagged primary antibodies for 1 hour at room temperature. Then, after one PBS wash, re-suspended the pellet in PBS, and filtered with cell strainer, and used those cells for FACS analysis using FACS AriaIII.

For analyzing the stem cell pool, oral cancer cells stably expressing ALDH1A1 DsRed2 (reporter cell line) with EPHA2/ Ephrin-B1 knock-down were trypsinized and re-suspended the pellet in PBS, and filtered with cell strainer, and analyzed in FACS AriaIII.

Co-Immunoprecipitation (Co-IP) experiments

We did conjugation of protein A/G bead with the specific antibody or IgG antibodies for 5 hours. We prepared cell lysate using lysis buffer (0.15 M Sodium chloride, 0.025M Tris, 0.001 M EDTA, 0.5% (v/v) NP40, 0.5% (v/v) Triton X 100, 5% glycerol (v/v), 1× protease inhibitor, pH 7.4). Cell lysate was quantified using DC protein assay (BioRad) and 1 mg precleared cell lysate was added to bead-antibody conjugate or bead-IgG conjugate and incubated overnight. The next day, protein-antibody complex was eluted using 5X loading dye. The eluate was used for western-blotting and probed for desired molecules.

ShRNA lentiviral particles and infection

The lentiviral particles for Scrambled and EPHA2 and Ephrin-B1 shRNA were purchased from Santa Cruz Biotechnology, Inc. This lentiviral particles contain a mixture of three target-specific constructs that encode 19-25 nucleotides (plus hairpin) shRNA designed to knock down

the expression of that specific gene. One day before infection, cells were seeded in a 24-well plate. On the day of infection, fresh medium containing 20ug/ml sequabrene was added to cells. Then, 6- 10×10^4 *ifu/ml* of viral shRNA particles were directly added to that medium. This infection procedure was repeated the next day as well. Then, the LV-shRNA infected cells were selected using puromycin antibiotic (200 ng/ml).

Extreme Limiting Dilution Assay (ELDA)

For in vitro sphere formation assay, cells were trypsinized and the serial dilutions were prepared and seeded in 96 well plate in sphere medium and maintained for 6 days with frequent medium change. On the 6th day, counted the spheres in each well and data was used for Extreme limiting dilution assay (ELDA, (https://bioinf.wehi.edu.au/software/elda/). CSC frequency was calculated using ELDA analysis, which is a webtool available online, and designed by the Bioinformatics Division, The Walter and Eliza Hall Institute of Medical Research in Australia. ELDA plotted a log-fraction plot, the slope of which gives CSC frequency.

For in vivo serial dilution xenograft assay, cells were serially diluted and mixed with growth factor-reduced matrigel and injected subcutaneously on the flanks of the mice. After 3 weeks, tumors were collected and representative images were taken. CSC frequency was calculated using ELDA.

Animal models for oral carcinoma

NOD.CB17-*Prkdc^{scid}*/J (SCID) or NOD.CB17-Prkdc^{scid}I12rg^{tm1Wjl}/SzJ (NSG) mice were used for generating tumors following approved protocols from IAEC. For in-vivo serial dilution xenograft assay, $1x10^6$ cells of oral cancer cells were mixed with growth factor-reduced matrigel and injected subcutaneously on the flanks of the mice. Tumors were collected after 2-3 weeks and

photographed. For the orthotopic model, $1x10^6$ cells of oral cancer cells were mixed with growth factor-reduced matrigel and injected to the floor of the mouth region superficial to the mylohyoid muscle. The animals were periodically monitored for overall survival analysis. The weight of the animals and tumor volume was measured periodically (using digital Vernier calipers) for 10 weeks. The death of the animal or ethical endpoint (visible signs of pain or distress or if the weight loss was >25% of pre-injection) was considered as the survival time.

Patient samples

Fresh Oral squamous cell carcinoma (OSCC) samples were collected from Regional Cancer Centre (RCC), Thiruvananthapuram, after getting written consent from the patients. Archival samples were collected from Cochin Cancer Research Centre (CCRC), Patients were categorized as recurrent and non-recurrent groups where patients with disease-free survival of less than 15 months were considered as recurrent (25 samples) while patients with disease free survival for more than 15 months were considered as non-recurrent group (27 samples).

***In-silico* analysis of oral cancer patient data**

To analyze the pattern of expression of EPHA2, Ephrin-B1, and EPHB2 mRNA in oral cancer specimens, data was downloaded from the Gene Expression Omnibus data portal (https://www.ncbi.nlm.nih.gov/geo/). The GEO accession numbers of the datasets are GSE13601, GSE65858. Platform used for expression profiling in all the three datasets were microarray. In GSE65858 a total of 300 samples were considered for analysis and quality control procedures were applied to microarray probe-level intensity files. A total of 255 tumor arrays remained after removing low-quality arrays, duplicate arrays, and arrays from non-HNSCC samples. Expression values were log2-transformed and normalized using RSN. The relative normalized log transformed

microarray data was used for all the analysis. The TCGA data (N=515) was accessed from the TCGA Research Network: https://www.cancer.gov/tcga (accessed on 15 November 2021).

Descriptive statistics were used for all clinical variables. The difference in gene expression levels was evaluated by the Mann–Whitney U test/Kruskal–Wallis test. Correlations were evaluated by Pearsons's rank test. Heatmap analysis was also performed to analyze association of various genes EPHA2, Ephrin-B1 and EPHB2. Kaplan-Meier analysis was used to examine the estimated differences in overall survival between the various groups. Log-rank test (Mantel-Cox) was used to compare the survival between groups. Survival analysis was performed by stratifying tumors based on the upper or third quartile expression of EPHA2 and Ephrin-B1 mRNA levels and grouped into tumors with high and low expression. For all tests, a p-value of <0.05 was considered to be statistically significant. All statistical analysis was carried out using the software XLSTAT - version 2022.2.1.

Tissue microarray (TMA) and IHC analysis

Immunohistochemistry for the antibodies was done on each of the TMA sections as per standard protocol using the Ventana Benchmark^{XT} staining system (Ventana Medical Systems, Tucson, AZ, USA). Briefly, 5 µm thick sections were fixed in a hot air oven at 60°C for 60 min and loaded on to an IHC staining machine. De-paraffinization was performed using EZ Prep solution (Proprietary-Ventana reagent), and antigen retrieval was done using Cell Conditioning solution 1 (CC1) for 60 min. The primary antibody was added manually and incubated for 32 min at room temperature. Optiview DAB Detection Kit (Ventana Medical Systems) was used to visualize the signal, using DAB (3–3′diaminobenzidine) as the chromogen. Further, the sections were automatically counterstained with hematoxylin II (Ventana Medical Systems) for 12 min. The

slides were removed from the autostainer, washed in de-ionized water, dehydrated in graded ethanol, cleared in xylene, and examined by microscopy. Appropriate positive and negative controls were run for each batch. Two pathologists scored the staining independently. Nuclear/cytoplasmic staining in more >1% of tumor cells was considered as positive. Data from 15 recurrent and 16 non-recurrent samples were used for the statistical analysis.

Data availability

All the data used for the proteomic analysis are provided as the supplementary tables. The source data of this paper collected in the following database records: The data analysed is publicly available. The data was downloaded from the Gene Expression Omnibus data portal (https://www.ncbi.nlm.nih.gov/geo/), and from the TCGA Research Network: https://www.cancer.gov/tcga.

References

Arthur A, Koblar S, Shi S, Gronthos S (2009) Eph/ephrinB mediate dental pulp stem cell mobilization and function. *J Dent Res* 88: 829-834

Arthur A, Nguyen TM, Paton S, Zannettino ACW, Gronthos S (2019) Loss of EfnB1 in the osteogenic lineage compromises their capacity to support hematopoietic stem/progenitor cell maintenance. *Exp Hematol* 69: 43-53

Bai J, Chen Y, Sun Y, Wang X, Wang Y, Guo S, Shang Z, Shao Z (2024) EphA2 promotes the transcription of KLF4 to facilitate stemness in oral squamous cell carcinoma. *Cell Mol Life Sci* 81: 278

Banki M, Moosavi MS (2023) Umbrella Review on Cancer Stem Cell in Oral and Head and Neck Squamous Cell Carcinoma. *J Stem Cells Regen Med* 19: 29-33

Batlle E, Henderson JT, Beghtel H, van den Born MM, Sancho E, Huls G, Meeldijk J, Robertson J, van de Wetering M, Pawson T *et al* (2002) Beta-catenin and TCF mediate cell positioning in the intestinal epithelium by controlling the expression of EphB/ephrinB. *Cell* 111: 251-263

Binda E, Visioli A, Giani F, Lamorte G, Copetti M, Pitter KL, Huse JT, Cajola L, Zanetti N, DiMeco F *et al* (2012) The EphA2 receptor drives self-renewal and tumorigenicity in stem-like tumor-propagating cells from human glioblastomas. *Cancer Cell* 22: 765-780

Castellvi J, Garcia A, de la Torre J, Hernandez J, Gil A, Xercavins J, Ramon y Cajal S (2006) Ephrin B expression in epithelial ovarian neoplasms correlates with tumor differentiation and angiogenesis. *Hum Pathol* 37: 883-889

Catchpole T, Henkemeyer M (2011) EphB2 tyrosine kinase-dependent forward signaling in migration of neuronal progenitors that populate and form a distinct region of the dentate niche. *J Neurosci* 31: 11472-11483

Chen K, Bai H, Liu Y, Hoyle DL, Shen WF, Wu LQ, Wang ZZ (2015) EphB4 forward-signaling regulates cardiac progenitor development in mouse ES cells. *J Cell Biochem* 116: 467-475

Davaatsend O, Altannamar M, Ganbat M, Jagdagsuren U (2024) Factors associated with recurrence in patients with oral cancer in Mongolia. *BMC Cancer* 24: 356

Dharmapal D, Jyothy A, Mohan A, Balagopal PG, George NA, Sebastian P, Maliekal TT, Sengupta S (2021) beta-Tubulin Isotype, TUBB4B, Regulates The Maintenance of Cancer Stem Cells. *Front Oncol* 11: 788024

Ebrahim AS, Hailat Z, Bandyopadhyay S, Neill D, Kandouz M (2021) The Value of EphB2 Receptor and Cognate Ephrin Ligands in Prognostic and Predictive Assessments of Human Breast Cancer. *Int J Mol Sci* 22

Falivelli G, Lisabeth EM, Rubio de la Torre E, Perez-Tenorio G, Tosato G, Salvucci O, Pasquale EB (2013) Attenuation of eph receptor kinase activation in cancer cells by coexpressed ephrin ligands. *PLoS One* 8: e81445

Gehring MP, Pasquale EB (2020) Protein kinase C phosphorylates the EphA2 receptor on serine 892 in the regulatory linker connecting the kinase and SAM domains. *Cell Signal* 73: 109668

Goichberg P, Bai Y, D'Amario D, Ferreira-Martins J, Fiorini C, Zheng H, Signore S, del Monte F, Ottolenghi S, D'Alessandro DA *et al* (2011) The ephrin A1-EphA2 system promotes cardiac stem cell migration after infarction. *Circ Res* 108: 1071-1083

Harsha HC, Pinto SM, Pandey A (2013) Proteomic strategies to characterize signaling pathways. *Methods Mol Biol* 1007: 359-377

Hu Y, Smyth GK (2009) ELDA: extreme limiting dilution analysis for comparing depleted and enriched populations in stem cell and other assays. *J Immunol Methods* 347: 70-78

Hu Y, Xie Q, Zhao J, Yang R, Qin J, Li H, Zhao Y, Du X, Shi C (2024) Interaction between the EPHB2 receptor and EFNB1 ligand drives gastric cancer invasion and metastasis via the Wnt/beta-catenin/FAK pathway. *Int J Biol Macromol* 258: 128848

Jain S, Dhall K, Brar GS, Gupta S, Jain K, Garg N, Sood S, Aggarwal R, Sidhu M (2024) Outcome of Upfront Surgically Resected Patients of Oral Tongue Squamous Cell Carcinoma and Factors Affecting it: Experience from Tertiary Care Facility in North India. *Indian J Otolaryngol Head Neck Surg* 76: 4479-4486

Jang BG, Kim HS, Chang WY, Bae JM, Kang GH (2018) Prognostic Significance of EPHB2 Expression in Colorectal Cancer Progression. *J Pathol Transl Med* 52: 298-306

Jeong WG, Choi H, Chae KJ, Kim J (2022) Prognosis and recurrence patterns in patients with early stage lung cancer: a multi-state model approach. *Transl Lung Cancer Res* 11: 1279-1291

Kakarla M, ChallaSivaKanaka S, Dufficy MF, Gil V, Filipovich Y, Vickman R, Crawford SE, Hayward SW, Franco OE (2022) Ephrin B Activate Src Family Kinases in Fibroblasts Inducing Stromal Remodeling in Prostate Cancer. *Cancers (Basel)* 14

Kalo MS, Yu HH, Pasquale EB (2001) In vivo tyrosine phosphorylation sites of activated ephrin-B1 and ephB2 from neural tissue. *J Biol Chem* 276: 38940-38948

Kim H, Myung JK, Paik SS, Kim H, Park H, Kim YJ, Lee SB, Kim HU, Song HJ, Jeong IH *et al* (2022) EPHB2 expression is associated with intestinal phenotype of gastric cancer and indicates better prognosis by suppressing gastric cancer migration. *Am J Cancer Res* 12: 1295-1308

Kristiansen TZ, Harsha HC, Gronborg M, Maitra A, Pandey A (2008) Differential membrane proteomics using 18O-labeling to identify biomarkers for cholangiocarcinoma. *J Proteome Res* 7: 4670-4677

Lechtenberg BC, Gehring MP, Light TP, Horne CR, Matsumoto MW, Hristova K, Pasquale EB (2021) Regulation of the EphA2 receptor intracellular region by phosphomimetic negative charges in the kinase-SAM linker. *Nat Commun* 12: 7047

Lee YJ, Jung SP, Bae JW, Yang SM, You JY, Bae SY (2023) Prognosis according to the timing of recurrence in breast cancer. *Ann Surg Treat Res* 104: 1-9

Leung HW, Leung CON, Lau EY, Chung KPS, Mok EH, Lei MML, Leung RWH, Tong M, Keng VW, Ma C *et al* (2021) EPHB2 Activates beta-Catenin to Enhance Cancer Stem Cell Properties and Drive Sorafenib Resistance in Hepatocellular Carcinoma. *Cancer Res* 81: 3229-3240

Li JY, Xiao T, Yi HM, Yi H, Feng J, Zhu JF, Huang W, Lu SS, Zhou YH, Li XH *et al* (2019) S897 phosphorylation of EphA2 is indispensable for EphA2-dependent nasopharyngeal carcinoma cell invasion, metastasis and stem properties. *Cancer Lett* 444: 162-174

Liu W, Yu C, Li J, Fang J (2022) The Roles of EphB2 in Cancer. *Front Cell Dev Biol* 10: 788587

Mann F, Harris WA, Holt CE (2004) New views on retinal axon development: a navigation guide. *Int J Dev Biol* 48: 957-964

Medori M, Spelzini G, Scicolone G (2020) Molecular complexity of visual mapping: a challenge for regenerating therapy. *Neural Regen Res* 15: 382-389

Mellitzer G, Xu Q, Wilkinson DG (1999) Eph receptors and ephrins restrict cell intermingling and communication. *Nature* 400: 77-81

Mencucci MV, Lapyckyj L, Rosso M, Besso MJ, Belgorosky D, Isola M, Vanzulli S, Lodillinsky C, Eijan AM, Tejerizo JC *et al* (2020) Ephrin-B1 Is a Novel Biomarker of Bladder Cancer Aggressiveness. Studies in Murine Models and in Human Samples. *Front Oncol* 10: 283

Miao H, Li DQ, Mukherjee A, Guo H, Petty A, Cutter J, Basilion JP, Sedor J, Wu J, Danielpour D *et al* (2009) EphA2 mediates ligand-dependent inhibition and ligand-independent promotion of cell migration and invasion via a reciprocal regulatory loop with Akt. *Cancer Cell* 16: 9-20

Mirshahidi S, Yuan IJ, Chen Z, Simental A, Lee SC, Andrade Filho PA, Murry T, Zeng F, Duerksen-Hughes P, Wang C *et al* (2024) Tumor Cell Stemness and Stromal Cell Features Contribute to Oral Cancer Outcome Disparity in Black Americans. *Cancers (Basel)* 16

Ottone C, Krusche B, Whitby A, Clements M, Quadrato G, Pitulescu ME, Adams RH, Parrinello S (2014) Direct cell-cell contact with the vascular niche maintains quiescent neural stem cells. *Nat Cell Biol* 16: 1045-1056

Pasquale EB (2010) Eph receptors and ephrins in cancer: bidirectional signalling and beyond. *Nat Rev Cancer* 10: 165-180

Pasquale EB (2024) Eph receptors and ephrins in cancer progression. *Nat Rev Cancer* 24: 5-27

Phan NN, Liu S, Wang CY, Hsu HP, Lai MD, Li CY, Chen CF, Chiao CC, Yen MC, Sun Z *et al* (2020) Overexpressed gene signature of EPH receptor A/B family in cancer patients-comprehensive analyses from the public high-throughput database. *Int J Clin Exp Pathol* 13: 1220-1242

Sawai Y, Tamura S, Fukui K, Ito N, Imanaka K, Saeki A, Sakuda S, Kiso S, Matsuzawa Y (2003) Expression of ephrin-B1 in hepatocellular carcinoma: possible involvement in neovascularization. *J Hepatol* 39: 991-996

Shanmugam G, Mohan A, Kumari K, Louis JM, Soumya Krishnan U, Balagopal PG, George NA, Sebastian P, Maliekal TT (2019) A novel reporter construct for screening small molecule inhibitors that specifically target self-renewing cancer cells. *Exp Cell Res* 383: 111551

Song W, Ma Y, Wang J, Brantley-Sieders D, Chen J (2014) JNK signaling mediates EPHA2-dependent tumor cell proliferation, motility, and cancer stem cell-like properties in non-small cell lung cancer. *Cancer Res* 74: 2444-2454

Stokowski A, Shi S, Sun T, Bartold PM, Koblar SA, Gronthos S (2007) EphB/ephrin-B interaction mediates adult stem cell attachment, spreading, and migration: implications for dental tissue repair. *Stem Cells* 25: 156-164

Wang B, Zhang S, Yue K, Wang XD (2013) The recurrence and survival of oral squamous cell carcinoma: a report of 275 cases. *Chin J Cancer* 32: 614-618

Xiang YP, Xiao T, Li QG, Lu SS, Zhu W, Liu YY, Qiu JY, Song ZH, Huang W, Yi H *et al* (2020) Y772 phosphorylation of EphA2 is responsible for EphA2-dependent NPC nasopharyngeal carcinoma growth by Shp2/Erk-1/2 signaling pathway. *Cell Death Dis* 11: 709

Yin Y, Yamashita Y, Noda H, Okafuji T, Go MJ, Tanaka H (2004) EphA receptor tyrosine kinases interact with co-expressed ephrin-A ligands in cis. *Neurosci Res* 48: 285-296

Zhao C, Wang A, Lu F, Chen H, Fu P, Zhao X, Chen H (2017) Overexpression of junctional adhesion molecule-A and EphB2 predicts poor survival in lung adenocarcinoma patients. *Tumour Biol* 39: 1010428317691000

Zhao H, Chen Z, Fang Y, Su M, Xu Y, Wang Z, Gyamfi MA, Zhao J (2022) Prediction of Prognosis and Recurrence of Bladder Cancer by ECM-Related Genes. *J Immunol Res* 2022: 1793005

Zhu L, Dissanayaka WL, Green DW, Zhang C (2015) Stimulation of EphB2/ephrin-B1 signalling by tumour necrosis factor alpha in human dental pulp stem cells. *Cell Prolif* 48: 231-238

Acknowledgements

We acknowledge Akhilesh Pandey and Proteomic facility of Institute of bioinformatics, Bangalore for the proteomic analyses. The contribution of Annie Agnes Suganya S for Fig 1C is acknowledged. We thank the contributions of the Animal Research Facility, the Confocal Facility and FACS Facility of RGCB. Reshma Raj R received funding from Council of Scientific & Industrial Research, India (09/716(0188)/2019-EMR-I). The work was financially supported by the funding from DST-SERB (SR/S0/HS/0133/2010), DBT (BT/PR14379/Med/30/536/2010) and RGCB LRF.

Author contributions

Reshma Raj R: Conceptualization; Formal analysis; Investigation; Writing - original draft; Writing - review and editing, Soumya Krishnan U: Investigation, Geetha Shanmugam: Investigation, Nandini Datta: Investigation; Writing—review and editing, Jiss Maria Louis: Conceptualization, Ravichandran Damodaran Jeyaram: Investigation, Keshava K Datta: Investigation; Data curation; Formal analysis, Harsha Gowda: Investigation; Data curation; Formal analysis, Meghna Sarkar: Investigation, Madhumathy G Nair: Investigation; Data curation; Formal analysis, Jyothy S Prabhu: Investigation, Hafsa Shabeer: Investigation, Balagopal P G: Resources, Thameem A: Resources, Alan Jose: Resources, and Tessy Thomas Maliekal: Conceptualization; Funding acquisition; Project administration; Supervision; Writing – review & editing.

Disclosure and competing interests

Authors declare no conflict of interest

Supplementary information accompanies the paper